Optically Induced Second Harmonic Generation by Six-wave Mixing: A Novel Probe of Solute Orientational Dynamics

Shujie Lin, Ian D. Hands, David L. Andrews, and Stephen R. Meech*

School of Chemical Sciences, University of East Anglia, Norwich NR4 7TJ, U.K.

Received: November 23, 1998; In Final Form: March 15, 1999

The optically induced generation of second harmonics in isotropic media, which arises through a six-wave mixing interaction, is employed in ultrafast studies of orientational relaxation in solution (4-diethylamino-4′-nitrostilbene in a range of solvents). It is shown that polar order can be induced in the samples by simultaneous irradiation at the fundamental and second harmonic frequencies. Time-resolved experiments in nonpolar solvents show that the polar order (which supports second harmonic generation) decays as a biexponential function of time. The two time constants are linearly dependent on viscosity and fall in the ratio 6:1. This result is shown to be consistent with a simple model of the six-wave mixing interaction incorporating orientational diffusion. The two relaxation components arise through contributions from the first and third moments of the solute orientational distribution function, confirmed by the polarization dependence of the time-resolved signal. Thus, it has been demonstrated that odd moments of the orientational distribution function, required for a complete description of molecular orientation, are accessible through six-wave mixing experiments; such data are not available in four-wave mixing measurements. The measurements have been extended to polar solvents, where the accelerated population relaxation of the solute is apparent. The dynamics at early times in polar solvents are complex, an effect which is explained in terms of a time-dependent molecular hyperpolarizability.

1. Introduction

In the past few years it has become apparent, from both theoretical and experimental investigations, that six-wave mixing (SWM) measurements provide access to information about molecular structure and dynamics that is not available from four-wave methods.[1−5] A particularly interesting example of a SWM signal is the generation of even harmonics from isotropic media, a process which is forbidden in lower order experiments.[6−9] The application of this SWM signal to an elucidation of the orientational dynamics of solutions is the subject of this paper, and it will be shown that new information is extracted from the measurement.

The experimental configuration to be described involves the simultaneous irradiation of the sample with femtosecond laser pulses at a fundamental frequency, ω and its second harmonic 2ω, followed by a time-delayed pulse at ω which generates a signal at 2ω. The effect of simultaneous irradiation of a sample at ω and 2ω has been described theoretically by several groups. The result is the generation of a degree of polar order in the sample.[8−10] The degree of polar order depends on the relative amplitudes of the two pulses and the phase difference between them. This latter factor makes possible a degree of coherent control of molecular orientation.[11,12] The fact that polar order is indeed generated in the sample is demonstrated by the observation that the sample supports second harmonic generation by a time-delayed pulse.[8,9,13−15] This was first demonstrated by Nunzi and co-workers, who have gone on to exploit the technique as a means of "optical poling" of polymers.[16−18]

Our objective in this paper is to demonstrate that observations of the induced second harmonic intensity as a function of delay time records the decay, through orientational diffusion, of the induced polar order in solution. In particular we will provide experimental verification that this time delayed signal yields odd moments ($l = 1$ and $l = 3$) of the orientational distribution function. The measurement of such odd orientational moments is important for a complete characterization of the orientational distribution function. Time domain four-wave mixing experiments, such as transient grating scattering, provide only the alignment moment $l = 2$.[19]

The paper is organized as follows. In the next section we will describe a new experimental configuration for the phase-matched SWM experiment, which is more suitable for ultrafast time-resolved measurements than the phase conjugate geometry previously employed.[6,8,9] Measurements of the SHG signal generated by a time delayed pulse from a solution of 4-diethylamino-4′-nitrostilbene (DEANS) are presented. It is shown that the experiment permits the collection of data with high signal-to-noise, suitable for detailed analysis. In the third section a simple description of the generation of polar order in isotropic media is given. The relationship between the different theoretical expressions for polar order, independently derived in the literature, is highlighted. The predictions of the theory for the time-resolved experiment are presented for different combinations of polarization and are compared with experimental measurements. In the case of nonpolar solvents the agreement between theory and experiment is very good. The viscosity dependence is shown to be consistent with the modified Stokes−Einstein−Debye model of rotational diffusion.[19−21] The more complex behavior in polar solvents is discussed in terms of solvent stabilization of internal charge transfer states and the effect this has on the molecular hyperpolarizability. The conclusions are drawn together in the final section.

* Author to whom correspondence may be addressed. E-mail: S.meech@uea.ac.uk.

10.1021/jp9845221 CCC: $18.00
Published on Web 05/05/1999

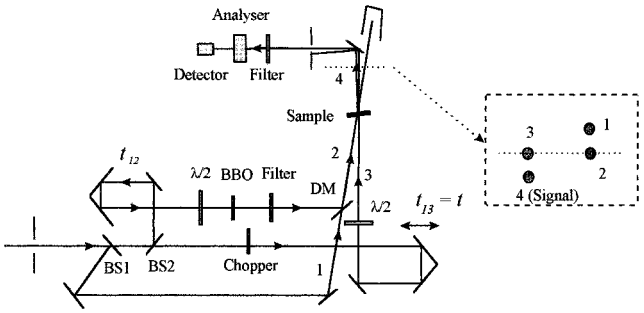

Figure 1. Block diagram of the experimental setup for the SWM experiment in the grating scattering configuration. In the inset the relative positions of the incident beams and signal beam (behind the sample) are shown. For a detailed description see text.

2. Measurement

The experimental geometry used in these experiments is shown in Figure 1. The light source was a regeneratively amplified Ti:Al_2O_3 laser (Clark-MXR CPA-1000) delivering sub-100 fs pulses at 800 nm with a repetition rate of 5 kHz. The output beam was passed through a half-wave plate and polarizer combination, to control power, and collimated and reduced in diameter to 0.8 mm using a telescope assembly. The beam polarization was set to vertical and the beam was divided at a 50% beamsplitter. The reflected beam (beam 1) was routed through a fixed optical path to the sample. The transmitted beam was further divided at a second beamsplitter with low reflectivity ($r \sim 3\%$). The weak reflected part (beam 2) passed through a translatable delay stage (t_{12}, accuracy 2 μm) and was then frequency doubled in a 300 μm thick BBO crystal. A half-wave plate was placed before the BBO crystal to rotate the incident 800 nm to horizontal polarization, so that the 400 nm radiation generated was vertically polarized (type I phase-matched second harmonic generation). The 400 nm beam was directed onto the sample via a dichroic mirror. The beam transmitted by the second beamsplitter (beam 3) was directed onto the sample through a motorized delay stage (t_{13}, positional accuracy 0.1 μm) and a half-wave plate. Beam 2 and beam 3 were incident in a horizontal plane and crossed at an angle of 4.5° in the sample. Beam 1 at 800 nm was positioned directly below beam 2, rising so as to cross beams 1 and 2 in the sample at an angle of 1° (see the inset of Figure 1). With the angles set as above there was a good spatial overlap of beams in the sample yet allowing the generated signal, beam 4, to be well separated from the transmitted beams for ease of detection. The temporal overlap between beams 1 and 2 was achieved by the observation of sum-frequency generation in a second BBO crystal located at the sample position. Using the cross-correlation trace between beams 1 and beam 2, the cross-correlation width at the sample was minimized to 100 fs by adjusting the compressor of the Ti:Al_2O_3 laser to compensate for the dispersion of glass in the optical path. With the compressor optimized, the pulses were close to transform limited. The final peak powers at the sample were 80 GW/cm^2 (beam 1), 0.2 GW/cm^2 (beam 2), and 75 GW/cm^2 (beam 3).

With this geometry, shown in Figure 1, the second-harmonic signal (beam 4) was emitted along the phase-matched direction defined by

$$\vec{k}_4(\omega) = 2\vec{k}_3(\omega) + [\vec{k}_2(2\omega) - 2\vec{k}_1(\omega)] \qquad (1)$$

where $\vec{k}_i$ is the wave vector for the ith beam (see also the inset to Figure 1). The geometry of Figure 1 differs from the phase conjugate geometry used previously[9] in which the pump (beam 1) and probe beam (beam 3) are counterpropagating. The advantage of the current geometry for ultrafast measurements is that the time resolution is no longer a function of the path length of the cell.[9,22] Thus the signal strength can be optimized by an appropriate choice of cell length without compromising time resolution. The signal was passed through a spatial filter, a band-pass filter, and an analyzing polarizer before detection by a monochromator/photomultiplier tube combination. The output of the photomultiplier was processed by a lock-in amplifier referenced to the frequency of a chopper placed in the path of beam 3. Both t_{13} and the lock-in were under computer control.

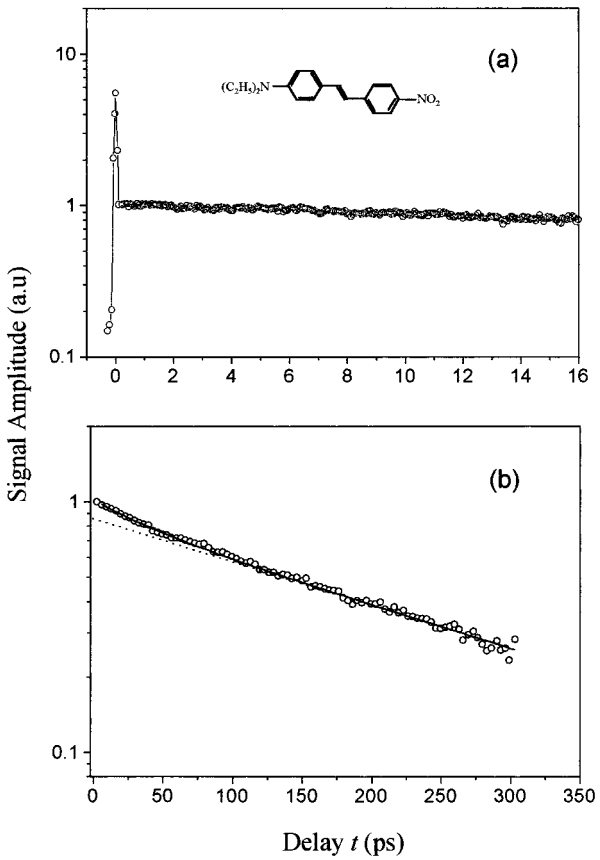

Figure 2. Amplitude of the six-wave mixing signal from the DEANS solution in mesitylene (the molecular structure of DEANS is shown inset). Data are shown as a function of the beam 3 delay $t \equiv t_{13}$. All fields are vertically polarized. (a) The data recorded at short times, with a coherence spike at $t = 0$ followed by a smooth decay. (b) The same data as (a) but on a longer time scale. The biexponential form of the relaxation is apparent and emphasized by the fit of a single-exponential function to the data at $t > 120$ ps (dotted line).

The samples were solutions of 4-diethylamino-4′-nitrostilbene (DEANS). DEANS was used because of its good solubility in nonpolar solvents relative to 4-dimethylamino-4′-nitrostilbene (DMANS), which was used in our previous experiments.[9] The DEANS absorption maximum is at 440 nm, weakly dependent on solvent. The solute concentration was typically 1×10^{-3} M and the pathlength of the cell was *ca* 30 μm, yielding an optical density ~0.6 at 400 nm. The 30 μm path length was chosen to optimize coherent generation of the second harmonic throughout the cell. This is limited by the coherence length of the pulses (ca 40 μm) and the interaction length which, in the case of toluene being the solvent, was calculated to be 210 μm.

Figure 2 shows the signal generated at 2ω measured as a function of delay t_{13} for a solution of DEANS in mesitylene. The delay t_{12} was set to zero, as in all measurements reported

here. (Since t_{13} is the only time delay varied in the present experiments the subscripts can now be dropped.) Time zero corresponds to all three pulses being overlapped in time. In Figure 2 all incident beams were vertically polarised and the vertical component of the signal was detected. The measured signal has a simple form, with a coherence spike at $t = 0$ (Figure 2a) where all three beams overlap, followed by a simple relaxation, which detailed analysis reveals to be biexponential (Figure 2b). This result is discussed further in the following section. Here we merely note that the intensity of the signal was observed to depend quadratically on the intensity of beams 1 and 3 and linearly on that of beam 2. This is consistent with a six-wave mixing mechanism, as confirmed by a detailed study of the polarization dependence of the signal.[23]

3. Discussion

3.1. Orientationally Selective Excitation. One of the interesting features of this experiment is the generation of second harmonic emission from an isotropic solution, which is of course forbidden in the conventional second-order measurement, $\omega + \omega \rightarrow 2\omega$. An understanding of the origin of this higher order second-harmonic signal is crucial for interpretation of the ultrafast dynamics measured in the time-resolved experiment. It will be shown that, at least for the case of a time-delayed pulse 3, the signal can be viewed as arising from the generation in the sample of an anisotropic orientational grating by simultaneous irradiation at ω and 2ω. The treatment given here follows closely that of Fiorini et al.[14]

Consider a noncentrosymmetric molecule which has an electronic resonance at 2ω characterised by a transition dipole, $\vec{\mu}$, which exhibits a change in dipole moment between its ground and excited state, $\Delta\vec{\mu}$. The solute molecule DEANS is a good example.[8,24,25] The DEANS molecule, located at some arbitrary point $\vec{R}$ in the solution, is exposed to pulses at ω and 2ω, with wave-vectors $\vec{k}_1(\omega)$ and $\vec{k}_2(2\omega)$ and initial phases φ_1° and φ_2°, respectively, such that it experiences a total electric field

$$\vec{E} = \vec{E}_1(\omega)\cos[\vec{k}_1(\omega)\cdot\vec{R} - \omega t + \varphi_1^\circ] + \vec{E}_2(2\omega)\cos[\vec{k}_2(2\omega)\cdot\vec{R} - 2\omega t + \varphi_2^\circ] \quad (2)$$

and it is noted that the resultant electric field is asymmetric.[26]

For present simplicity a classical representation is employed. The quantum electrodynamical status of the phase in such a situation is an intricate issue which is currently the subject of further research.[27]

The probability of electronic excitation is given by $P_{10} = |a^{(1)}(2\omega) + a^{(2)}(\omega)|^2$, where $a^{(1)}(2\omega)$ and $a^{(2)}(\omega)$ are obtained from time-dependent perturbation theory (first- and second-order respectively)[26] as

$$a^{(1)}(2\omega) = \left(\frac{i\tau_p}{2\hbar}\right)[\vec{\mu}\cdot\vec{E}_2(2\omega)]e^{i[\vec{k}_2(2\omega)\cdot\vec{R}+\varphi_2^\circ]} \quad (3)$$

$$a^{(2)}(\omega) = \left(\frac{i\tau_p}{4\hbar^2\omega}\right)[\Delta\vec{\mu}\cdot\vec{E}_1(\omega)][\vec{\mu}\cdot\vec{E}_1(\omega)]e^{i[2\vec{k}_1(\omega)\cdot\vec{R}+2\varphi_1^\circ]} \quad (4)$$

corresponding to one- and two-photon interactions of beams 2 and 1, respectively, with the solute. In (3) and (4), τ_p is the pulsewidth. The resulting excitation probability consists of three terms:

$$P_{10} = b_1[\vec{\mu}\cdot\vec{E}_2(2\omega)]^2 + b_2[\Delta\vec{\mu}\cdot\vec{E}_1(\omega)]^2[\vec{\mu}\cdot\vec{E}_1(\omega)]^2 + b_3[\Delta\vec{\mu}\cdot\vec{E}_1(\omega)][\vec{\mu}\cdot\vec{E}_1(\omega)][\vec{\mu}\cdot\vec{E}_2(2\omega)]\cos(\Delta\varphi) \quad (5)$$

where $\Delta\varphi$ is

$$\Delta\varphi = [\vec{k}_2(2\omega) - 2\vec{k}_1(\omega)]\cdot\vec{R} + (\varphi_2^\circ - 2\varphi_1^\circ) \quad (6)$$

and the constants b_i involve ω and τ_p. The first two terms in (5) essentially correspond to the probability of one-photon absorption from beam 2 and two-photon absorption from beam 1. They contain no spatial part and so cannot contribute to grating scattering. More importantly the resulting orientational distribution of excited states (and ground states) is, for both terms, symmetrical with respect to inversion (see below), and so cannot support second-harmonic generation. Crucially, this is not the case with the third term in equation (5), in which the probability of excitation depends on both the position and orientation of the molecule with respect to the incident radiation. For example in the case of linearly polarized beams 1-3, this term yields $\Delta\mu\mu^2[E^2_1(\omega)E_2(2\omega)|\cos^3\theta\cos\Delta\varphi$, where θ is the angle between the molecular transition dipole and the polarization direction. The presence of the $\cos^3\theta$ term means that the excitation probability depends on the polar direction of the solute, i.e., molecules with a transition dipole pointing in one orientation with respect to the polarization direction are more likely to be excited than those with the opposite orientation. This orientationally selective excitation lifts the inversion symmetry of the sample so that the medium effectively has a finite $\chi^{(2)}$ and second-harmonic generation is allowed.

The spatial dependence is contained in the phase difference factor, eq 6. When the angle between beams 1 and 2 is nonzero, propagation through the sample causes a spatial modulation of the noncentrosymmetric excitation probability, with the result that a three-dimensional orientational $\chi^{(2)}$ grating is formed, with a grating vector $\vec{G} = \vec{k}_2(2\omega) - 2\vec{k}_1(\omega)$. This is responsible for the generation of a phase matched signal in the direction indicated by (1).

An equation very similar to (5) was derived earlier by Fiorini et al.[14] and applied in their studies of optical poling of polymers.[16−18] Relations closely related to (5) have also been derived by several other groups considering the effect of simultaneous irradiation at ω and 2ω. Most often the experimentally straightforward case of co-propagation of ω and 2ω has been considered. In that case, neglecting dispersion, $\vec{k}_2(2\omega) = 2\vec{k}_1(\omega)$ and the generation of asymmetry relies on the relative phase of the two pulses $\varphi_2^\circ - 2\varphi_1^\circ$. In such cases control of the relative phase by, for example, introducing a dispersive medium of varying length into the optical path yields a mechanism of coherent control. This aspect has been discussed in relation to photoionisation,[26,28,29] molecular orientation,[12] and photocurrent generation.[30,31] Brown and Meath also obtained an expression closely related to (5), employing rotating wave approximation methods, more appropriate for long pumping times, rather than perturbation theory.[10] Their results were discussed in relation to the coherent control of excited state population. In recent papers[32,33] Cho and co-workers have described a (fifth-order) nonresonant coherent hyper-Raman scattering experiment in which it was also shown that simultaneous irradiation by beams at ω and 2ω, with an angle between them, results in a grating which supports second-harmonic generation. Most recently of all we have employed the methods of molecular quantum electrodynamics to derive an expression which has the same orientational, intensity and spatial dependence as (5).[34]

From this collection of results it would seem that the theoretical description of the simultaneous interaction of two pulses at ω and 2ω in an isotropic medium is rather complete, while experimental observations are restricted to a few groups.[8,9] Below it will be shown that ultrafast time-resolved measure-

ments of the relaxation of the optically induced orientational grating yield new information on the orientational distribution function of molecules in solution.

Finally in this section it should be noted that the above analysis in terms of a $\chi^{(2)}$ grating induced by beams 1 and 2, and probed by beam 3, is not complete when all three beams are temporally overlapped. In that case the distinction between pump and probe beams cannot be made. For example, the $\chi^{(2)}$ grating can also be produced by interference between beams 2 and 3, such that SHG from beam 1 contributes to the measured signal. There is also the possibility of interference between beams 1 and 3, of the same frequency, to create additional gratings.[35] It is found that in this case a second-order scattering of beam 2 propagates along the same direction as the second harmonic from the $\chi^{(2)}$ grating. This final contribution dominates the time zero signal. This signal is not detected in the phase conjugate geometry, which shows a correspondingly weaker time zero signal.[9]

3.2. SWM Measurements of Orientational Dynamics. The SHG signal generated from beam 3 at time t reflects the decay of the induced $\chi^{(2)}$ grating. This may occur both through relaxation of excited state population and randomisation of solute orientation. Since the excited state lifetime of DEANS is long in nonpolar solvents (the lifetime in benzene is 3.3 ns[36]), relaxation by orientational diffusion will be considered first. The following simplifying assumptions will be made in the analysis concerning DEANS. First the molecular shape is taken as an extended ellipsoid. Secondly the only significant nonzero component of the molecular hyperpolarizability is assumed to lie along the long molecular axis, along which the transition dipole μ, is also polarized. While these are severe assumptions, they are fully justified both by the data (see below) and with respect to the structure of DEANS, which is indeed a long chain molecule with its transition moment dominated by the charge transfer transition along the long axis.[24,25] None of these assumptions is strictly necessary, and development of the theory for the SWM signal with molecules of arbitrary shape is in progress.[34]

The contribution to the second-harmonic signal of a single molecule in the solution irradiated in the manner described in section 3.1 is proportional to $[\hat{\mu}\cdot\hat{e}_4(2\omega)][\hat{\mu}\cdot\hat{e}_3(\omega)E_3(\omega)]^2\,\Delta\beta$,[37] where $\hat{e}_3$ and $\hat{e}_4$ are respectively the probe and signal polarization vectors, $\Delta\beta$ is the change in molecular first hyperpolarizability on excitation, and $\hat{\mu}\cdot\hat{e}_i$ represents the projection factor of the nonzero β along $\hat{\mu}$ on $\hat{e}_i$. The total response of the medium can thus be expressed as

$$E_4(2\omega,t) \propto \int [\hat{\mu}\cdot\hat{e}_4(2\omega)][\hat{\mu}\cdot\hat{e}_3(\omega)E_3(\omega)]^2 \Delta\beta N_1(t)\rho(\theta,\phi,t)\sin\theta\,\mathrm{d}\theta\,\mathrm{d}\phi$$

$$= N_1(t)\Delta\beta E_3^2(\omega)\int [\hat{\mu}\cdot\hat{e}_4(2\omega)][\hat{\mu}\cdot\hat{e}_3(\omega)]^2 \rho(\theta,\phi,t)\sin\theta\,\mathrm{d}\theta\,\mathrm{d}\phi \quad (7)$$

where $N_1(t)$ is the time-dependent population of the excited state and $\rho(\theta,\phi,t)$ the time-dependent orientational distribution function. The integration in (7) is over the originally randomly oriented molecules at point $\vec{R}$; integration across the spatial position in the medium has been omitted, since it merely defines the diffraction direction of the signal as has been discussed above (1), and has no effect on the measured relaxation dynamics.

The molecular orientation distribution has an initial distribution $\rho(\theta,\phi,t{=}0) = P_{10}$ as given by (5). Substitution of either of the first two terms of (5) in (7) leads to $E_4(2\omega,t) = 0$, which is consistent with the previous discussion based on symmetry. Conversely substitution of the third term in (5) into (7) leads to a finite result. Therefore only the relaxation of the distribution function given by the third term in (5) has to be considered in the present analysis.

With the assumptions concerning the structure of DEANS mentioned above the rotational diffusion is characterised by a single diffusion coefficient Θ about an axis perpendicular to the long molecular axis. The time dependence of the orientational distribution is then obtained, from a solution of the Debye equation by standard methods, as

$$\rho(\theta,\phi,t) \propto \sum\{\int [\Delta\vec{\mu}\cdot\vec{E}_1(\omega)][(\vec{\mu}\cdot\vec{E}_1(\omega)][\vec{\mu}\cdot\vec{E}_2(2\omega)] Y^*_{lm}(\theta',\phi')\sin\theta'\mathrm{d}\theta'\mathrm{d}\phi'\}\cdot Y_{lm}(\theta,\phi)\mathrm{e}^{-l(l+1)\Theta t} \quad (8)$$

where the $Y_{lm}(\theta,\phi)$ are the spherical harmonic functions which define the moments of the orientational distribution.[38] Only the terms with $l = 1$ and $l = 3$ are nonzero, because $[\Delta\vec{\mu}\cdot\vec{E}_1(\omega)][\vec{\mu}\cdot\vec{E}_1(\omega)][\vec{\mu}\cdot\vec{E}_2(2\omega)]$ is an odd function with respect to molecular orientation, requiring it to be described by odd spherical harmonics. The highest order in theta is $\cos^3\theta$, so that only terms up to $l = 3$ are allowed. This is true regardless of the polarization states of the pump fields. Thus we find

$$\rho(\theta,\phi,t) \propto E_1^2(\omega)E_2(2\omega)\mu^2 \Delta\mu\{[\sum c_{1m}Y_{1m}(\theta,\phi)]\mathrm{e}^{-2\Theta t} + [\sum c_{3m}Y_{3m}(\theta,\phi)]\mathrm{e}^{-12\Theta t}\} \quad (9)$$

where c_{lm} are polarization-dependent coefficients,

$$c_{lm} = \int (\hat{\mu}\cdot\hat{e}_1)^2(\hat{\mu}\cdot\hat{e}_2)Y^*_{lm}(\theta',\phi')\sin\theta'\mathrm{d}\theta'\mathrm{d}\phi' \quad (10)$$

Finally substitution of (9) into (7) and integration over (θ,ϕ) yields the following expression for E_4;

$$E_4(2\omega,t) \propto E_1^2(\omega)E_2(2\omega)E_3^2(\omega)\mu^2\Delta\mu(d_1\mathrm{e}^{-2\Theta t} + d_3\mathrm{e}^{-12\Theta t}) \quad (11)$$

Here d_l ($l = 1, 3$) are again polarization-dependent coefficients.[39] In (11) the six-wave mixing nature of the whole pump−probe process is obvious from the dependence of the signal amplitude on the incident fields; this has been confirmed by experiment. The signal is also dependent on the oscillator strength and the change in permanent dipole moment on excitation $\Delta\mu$.

The effect of the rotational relaxation on the decay of the measured signal, $\sqrt{I_4(2\omega,t)} \propto E_4(2\omega,t)$, lies in the term within the brackets in (11), which always contains a sum of $\mathrm{e}^{-2\Theta t}$ and $\mathrm{e}^{-12\Theta t}$ with their relative weight being polarization dependent. This model is then consistent with the biexponential behavior observed in Figure 2. This is an interesting result, as it shows that, by employing an anisotropic excitation scheme (5), it is possible to access experimentally odd moments ($l = 1$ and 3 in this case) of the orientational distribution function, and observe their relaxation on an ultrafast time scale. However, since there are many possible contributions to a nonexponential relaxation in a complex molecule, such as DEANS, the remainder of this section is concerned with proving that relations (7−11) apply.

Two polarization arrangements were considered. The first arrangement was with all beams 1−4 vertically polarized (Figure 2), for which (7−11) predicts

$$E_4'(2\omega,t) \propto 4\mathrm{e}^{-12\Theta t} + 21\mathrm{e}^{-2\Theta t} \quad (12)$$

The second arrangement is with beams 1 and 2 vertically

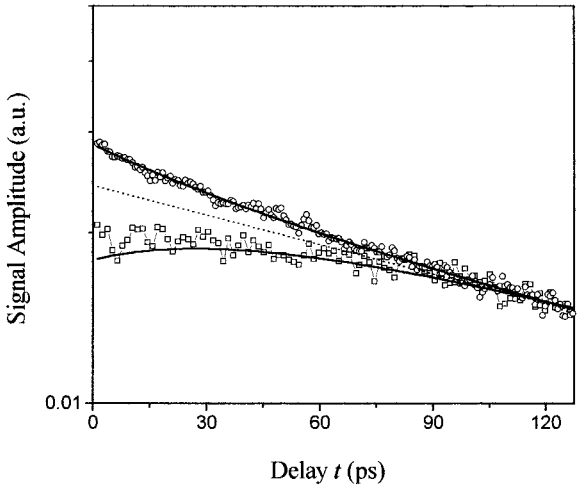

Figure 3. The time-dependence of the signal amplitudes with the two different polarization arrangements for a DEANS solution in mesitylene: (○) are the measured data for all vertical polarizations and (□) for vertical beams 1 and 2, beam 3 at 45°, and detection of the horizontal component of beam 4. The different dynamics are well fitted by (12) and (13) (solid lines) with the assumption of a single rotational diffusion coefficient, $\Theta = 2.0 \times 10^{-3}$ ps^{-1}. The dotted line is a single-exponential fit to the data at $t > 120$ ps.

polarized, beam 3 set at 45° and the analyser set to measure the horizontal component of beam 4. Equations 7−11 then yield

$$E_4''(2\omega,t) \propto -2e^{-12\Theta t} + 7e^{-2\Theta t} \qquad (13)$$

In Figure 2b the measured decay of $E_4'(2\omega,t)$ at positive time down to 300 ps is shown for a DEANS solution in mesitylene. The data was fitted to (12) using $\Theta = 2.0 \times 10^{-3}$ ps^{-1} (the two time constants are then $\tau_1 = 1/12\Theta = 41$ ps, $\tau_2 = 1/2\Theta = 246$ ps). The good agreement of measured and calculated data suggests that the predicted 6:1 ratio of relaxation times is operative and that molecular reorientation is indeed the mechanism of relaxation of $E_4(2\omega,t)$ in a nonpolar solvent.

A more stringent test of the model is the dependence of the measured dynamics on the polarization. Equations 12 and 13 reveal that at long times ($t \gg 1/2\Theta$) the time dependence of $E_4(2\omega,t)$ is controlled by $l = 1$, the lower moment of the orientational distribution. Then all polarizations produce the same dynamics. The behavior is, however, very different at short times ($t \leq 1/12\Theta$) where the third moment ($l = 3$) makes a significant contribution to the relaxation. In the case of all vertical polarizations the contribution of $1/12\Theta$ is positive and appears as a fast decay in the time evolution of the signal. In the second case the $1/12\Theta$ contribution is opposite in sign, creating a rising feature in the signal at short time. The measurements with these two polarization arrangements are shown in Figure 3.

Once the value of Θ has been measured accurately from $E_4'(2\omega,t)$ (Figure 2) there are no variable parameters in the analysis of $E_4''(2\omega,t)$. Taking that into account, and recalling the simplifying assumptions made concerning electronic structure and shape of DEANS, the agreement shown in Figure 3 is remarkably good. Thus we conclude that the time-resolved six-wave mixing experiment described provides a reliable means of accessing the first and third moments of the molecular orientational distribution function.

The value of the diffusion coefficient Θ extracted from the analysis via the relation $\tau_l = [l(l+1)\Theta]^{-1}$, has been obtained for a range of nonpolar solvents of differing viscosity. The result of a SWM measurement with all parallel polarizations in two

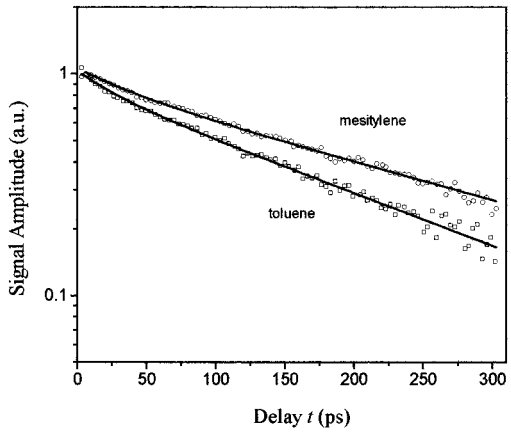

Figure 4. SWM signal amplitudes from the DEANS solutions in mesitylene (○) and toluene (□) as functions of the delay time. Data recorded with all vertical polarizations. The decay is clearly slower in the more viscous solvent. The solid curves are the dynamics predicted by the orientational relaxation model with $\Theta = 2.0 \times 10^{-3}$ ps^{-1} and $\Theta = 2.70 \times 10^{-3}$ ps^{-1} for mesitylene and toluene, respectively. Note that the time zero signal is not resolved in these lower time-resolution measurements.

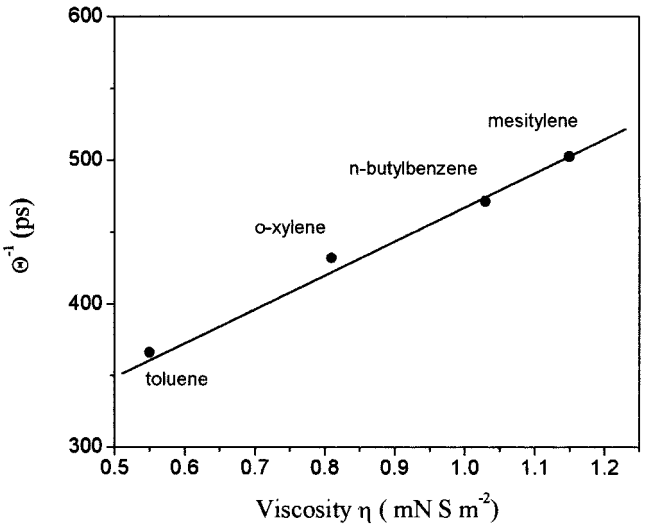

Figure 5. The viscosity dependence of the reciprocal of the diffusion coefficient, Θ^{-1}. The solid line is a linear fit to the data using (14). The slope is 2.3×10^2 ps/(mN s m^{-2}).

such solvents is shown in Figure 4. As can be seen both τ_l values increase with increasing viscosity. This is consistent with the predictions of the modified Stokes−Einstein−Debye model of orientational diffusion,[19−21] in which

$$\Theta^{-1} = \frac{6V_m fc}{kT}\eta + \Theta_0^{-1} \qquad (14)$$

where V_m is the molecular volume, f the shape factor given by Perrin,[40] c is a factor dependent on the hydrodynamic boundary condition (stick or slip), and Θ_0 is the value of the diffusion coefficient as $\eta \rightarrow 0$, sometimes interpreted as the free rotor frequency.[20] All solutions were sufficiently dilute for any corrections due to pair correlation to be safely neglected.[41]

Equation 14 predicts a linear relationship between Θ^{-1} and η, which is as observed for the series of nonpolar solvents shown in Figure 5; the slope was measured as 2.3×10^2 ps/(mN s m^{-2}). From the molecular structure and the van der Waals radii the asphericity parameter of a DEANS molecule is 0.30. This yields $f = 1.5$ and $c = 0.51$, so that the molecular volume

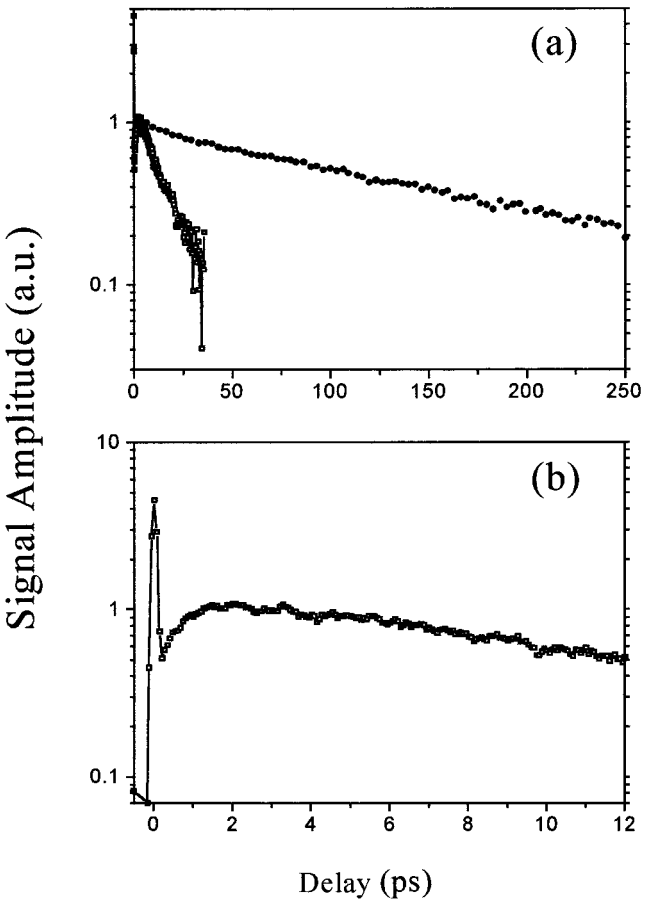

Figure 6. SWM signal amplitudes from the DEANS solutions in acetonitrile as functions of the delay time. Data recorded with all vertical polarizations: (a) The long time scale data (□) which shows a rapid relaxation with a decay time constant of 13.2 ps. For comparison the much slower relaxation in mesitylene (●) is shown. (b) The data recorded at short time, with a coherence spike and a rapid rise evident.

obtained from experiment is 208 Å^3. This can be compared with a calculation of the molecular volume of 280 Å^3 from the van der Waals increment method.[42] The agreement between measured and calculated volumes is reasonable, especially when it is recalled that the commonly used van der Waals increment method tends to overestimate molecular volumes, compared to, for example, Stuart−Briegleb space-filling models (by as much as 25% in the case of biphenyl).[19,20] However, less than quantitative agreement in measured and calculated V_m may also indicate that some of the approximations made in simplifying the diffusion tensor and the electronic structure of DEANS are not fully justified. This point will be investigated in a complete treatment of orientational relaxation observed through SWM for molecules of arbitrary shape.[34] However, we conclude from the good agreement between theory and experiment in Figures 3 and 5 that SWM in nonpolar solvents properly registers orientational dynamics, and that contributions from the first and third moments of the orientational distribution function are detected.

3.3. SWM Dynamics in Polar Solvents. In polar solvents the dynamics reported by the SWM measurement are complex and cannot be described by a simple orientational diffusion model. The experimental results are summarized in Figure 6 for the solvent acetonitrile. In all measurements the polarization of all beams was vertical. Figure 6a shows that the relaxation rate is greatly accelerated in acetonitrile. This is readily understood as a result of fast $S_1 \rightarrow S_0$ population relaxation, and the data are well fitted by (7) where $N_1(t) \propto \exp(-t/13.2$ ps). Such a short excited state lifetime for aminonitrostilbene (ANS) derivatives, including DEANS, has been suggested before on the basis of the low fluorescence quantum yield.[43] Lapouyade et al. suggested that polar solvents stabilise the formation of a nonradiative internal charge transfer (ICT) state. The formation of the ICT state is thought to involve an excited state conformational change, probably rotation about the nitro group bond.[43] The new data available from Figure 6a suggests that this process results in a rapid repopulation of the ground state, rather than population of a nonradiative bottleneck state. If relaxation to a bottleneck state occurred the SWM signal would still be generated from the orientational hole in the ground state population.

When viewed under higher time resolution the SWM dynamics in acetonitrile reveal a rapid risetime, never observed in nonpolar solvents (Figure 6b). A similar risetime was observed when acetone was the solvent, and with a THF solvent a rapid rise followed by a fast decay was reported in our earlier work.[9] The observed risetime is too rapid to be associated with diffusional orientational dynamics. A nondiffusive solute orientational (librational) motion could give rise to a fast component in SWM, but would be expected to appear in nonpolar solvents as well. As an alternative explanation we suggest that the fast-solvent dependent dynamics shown in Figure 6b have their origin in intramolecular relaxation, reflected in a time dependent molecular hyperpolarizability.

In the analysis presented in sections 3.1 and 3.2 it was assumed that DEANS comprises a ground and excited state which possess different hyperpolarisabilities. In reality at least the three lowest electronic states of DEANS contribute to the hyperpolarizability.[25] This will not influence the SWM measurements so long as the only effect of electronic excitation is to instantaneously shift population between these three levels, giving rise to a finite, but time independent, $\Delta\beta$ (7); this appears to be the case with nonpolar solvents. However, in polar solvents the nature and energy of the excited electronic states evolve with time. In particular polar solvent reorganization stabilizes ICT states. This will give rise to an evolution in dipole moment and transition dipole, which will in turn result in a time-dependent $\Delta\beta$. In addition, as a result of the formation of these polar ICT states the solvent relaxation causes large shifts in the energy of the excited state. For example the increase in Stokes shift between nonpolar and polar solvents like acetone is >3000 cm^{-1}.[43] Such large shifts in the frequency of resonant transitions will lead to a time-dependent hyperpolarizability. Both of these factors will contribute to the complex kinetics observed in polar solvents (Figure 6b and ref 9).

4. Conclusion

The application of ultrafast time-resolved SHG to the measurement of orientational dynamics in solution has been described. A simple model for the optically induced SHG has been outlined. Some features of the model, such as orientation-selective excitation and the possibility of a phase-controlled orientational distribution have been highlighted.

The relaxation of the initially prepared orientational distribution of solutes by orientational diffusion has been described. Experimental tests of the predictions of the model for a simple one-dimensional diffuser demonstrated that, at least in nonpolar solvents, the relaxation of the SHG with time occurs through orientational diffusion. The polarization-resolved measurements showed that the SWM experiment reveals the dynamics of the first and third ($l = 1$ and $l = 3$) moments of the orientational distribution function. These odd moments are not accessible

through four wave mixing experiments but are required for a complete description of solute orientation.

Additional measurements made in polar solvents have revealed SWM dynamics very different to the nonpolar case. This is consistent with literature data on the complex polar solvent-dependent excited state chemistry of ANS derivatives. The fast relaxation observed in polar solvents was assigned to $S_1 \rightarrow S_0$ population relaxation, while the rapid initial rise observed in the SHG was tentatively ascribed to a time-dependent molecular hyperpolarizability.

Acknowledgment. The authors would like to thank EPSRC for financial support.

References and Notes

(1) Barbara, P. F., Fujimoto, J. G., Knox, W. H., Zinth, W., (Eds.) *Ultrafast Phenomena X*; Springer Series in Chemical Physics, Vol. 62, Springer: Berlin, 1996.
(2) Tanimura, Y.; Mukamel, S. *J. Chem. Phys*. **1993**, *99*, 9496.
(3) Tominaga, K. ; Yoshihara, K. *Phys. Rev. Lett.* **1995**, *74*, 3061.
(4) Tominaga, K.; Yoshihara, K. *J. Chem. Phys.* **1996**, *104*, 4419.
(5) Steffen, T. ; Duppen, K. *Phys. Rev. Lett*. **1996**, *76*, 1224; *J. Chem. Phys*. **1997**, *106*, 3854.
(6) Ducloy, M. *Appl. Phys. Lett*. **1985**, *46*, 1020.
(7) Andrews, D.L. *Nonlinear Opt.* **1994**, *8*, 25.
(8) Charra, F.; Devaux, F.; Nunzi, J.-M.; Raimond, P. *Phys. Rev. Lett*. **1992**, *68*, 2440.
(9) Lin, S.; Hands, I. D.; Andrews, D. L.; Meech, S. R. *Chem. Phys. Lett*. **1998**, *285*, 321.
(10) Brown, A.; Meath, W. *J. Chem. Phys*. **1995**, *198*, 91.
(11) Fiorini, C.; Charra, F.; Nunzi, J.- M; Raimond, P. *J. Opt. Soc. Am*. B **1997**, *14*, 1984.
(12) Vrakking, M. J. J.; Stolte, S. *Chem. Phys. Lett.* **1997,** *271*, 209.
(13) Fiorini, C.; Nunzi, J.-M.; Charra, F.; Kajzar, F.; Lequan, M.; Lequan, R.-M.; Chane-Ching, K. *Chem. Phys. Lett.* **1997**, *335*, 271.
(14) Fiorini, C.; Charra, F.; Nunzi, J.-M. *J. Opt. Soc. Am. B* **1994**, *11*, 2347.
(15) Markovitsi, D.; Sigal, H.; Ecoffet, C.; Millie, P.; Charra, F.; Fiorini, C.; Nunzi, J.-M.; Strzelecka, H.; Veber, M.; Jallabert, C. *Chem. Phys*. **1994**, *182*, 69.
(16) Charra, F.; Kajzar, F.; Nunzi, J.-M.; Raimond, P.; Idiart, E. *Opt. Lett.* **1993**, *18*, 941.
(17) Fiorini, C.; Charra, F.; Raimond, P.; Lorin, A.; Nunzi, J.-M. *Opt. Lett*. **1997**, *22*, 1846.
(18) Fiorini, C.; Nunzi, J.-M. *Chem. Phys. Lett*. **1998**, *286*, 415.
(19) Deeg, F. W.; Stankus, J. J.; Greenfield, S. R.; Newell, V. J. ; Fayer, M. D. *J. Chem. Phys*. **1989**, *90*, 6893.
(20) Bauer, D. R.; Brauman, J. I.; and Pecora, R. *J. Am. Chem. Soc*. **1974**, *96*, 6840.
(21) Kivelson, D. In *Rotational Dynamics of Small and Macromolecules in liquids*; Dorfmuller, T., Pecora, R., Eds.; Springer Verlag: Berlin, 1987; p 1.
(22) Zhao, M.; Cui, Y.; Samoc, M.; Prasad, P. N.; Unroe, M. R.; Reinhardt, B. A. *J. Chem. Phys.* **1991**, *95*, 3991.
(23) Hands, I. D.; Lin, S.; Meech, S. R.; Andrews, D. L. *J. Chem. Phys*. **1998**, *109*, 10580.
(24) Beljonne, D.; Bredas, J. L.; Chen, G.; Mukamel, S. *Chem. Phys.* **1996**, *210*, 353.
(25) Beljonne, D.; Bredas, J. L.; Cha, M.; Torruellas, W. E.; Stegeman, G. I.; Hofstraat, J. W.; Horsthius, W. H. G.; Mohlmann, G. R. *J. Chem. Phys.* **1995**, *103*, 7834.
(26) Barranova, N. B.; Chudinov, A. N.; Zel'dovich, B. Y. *Opt. Commun*. **1990**, *79*, 116.
(27) Thirunamachandran, T.; Meath, W. J.; Andrews, D. L. Work in progress.
(28) Brumer, P.; Shapiro, M. *Chem. Phys. Lett*. **1986**, *126*, 541.
(29) Zhu, L.; Kleimam, V.; Li, X.; Lu, S.; Trentelman, K.; Gordon, R. J. *Science* **1995**, *270*, 77.
(30) Atanasov, R.;. Hache, A.; Hughes, J. L. P.; van Driel, H. M.; Sipe J. E. *Phys. Rev. Lett*. **1996**, *76*, 1703.
(31) Hache, A.; Kostoulas, Y.; Atanasov, R.; Hughes, J. L. P.; Sipe, J. E.; van Driel, H. M. *Phys. Rev. Lett.* **1997**, *78*, 306.
(32) Cho, M. *J. Chem. Phys*. **1997**, *106*, 7550.
(33) Yang, M.; Kim, J.; Jung, Y.; Cho, M. *J. Chem. Phys*. **1998**, *108*, 4013.
(34) Hands, I. D.; Lin, S.; Meech, S. R.; Andrews, D. L. In preparation.
(35) Fiorini, C.; Nunzi J.-M. *J. Opt. Soc. Am. B* **1991**, *8*, 570.
(36) Kobayashi, T.; Ohtani, H.; Kurohawa, K. *Chem. Phys. Lett*. **1985**, *121*, 356.
(37) Shen, Y. R. *Principles of Nonlinear Optics* Wiley: New York, 1984.
(38) Bain, A. J.; Chandna, P.; Butcher, G. *Chem. Phys. Lett*. **1996**, *260*, 441.
(39) $d_l = \sum \int c_{lm}[\hat{\mu} \cdot \hat{e}_4(2\omega)][(\hat{\mu} \cdot \hat{e}_3(\omega)]^2 Y_{lm}(\theta,\phi) \sin\theta \, d\theta \, d\phi$
(40) Perrin, F.; *Phys. Radium* **1934**, *5*, 497.
(41) Keyes, T.; Kivelson, D. *J. Chem. Phys.* **1980**, *72*, 5333.
(42) Edward, J. T. *J. Chem. Educ*. **1970**, *47*, 261.
(43) Lapouyade, R.; Kuhn, A.; Letar, J.-F; Rettig, W. *Chem. Phys. Lett*. **1993**, *208*, 48.